Ophthalmic Robot

David Larsson, Daniel Irving, Shehryar Effendi, Joshua Dubin, Austin Bach[1], Melissa Morris, Sabri Tosunoglu

Department of Mechanical and Materials Engineering
Florida International University
Miami, Florida

[1] TYB, Inc.
Miami Beach, Florida

dlars014@fiu.edu, dirvi004@fiu.edu, seffe001@fiu.edu, jdubi006@fiu.edu, mmorr009@fiu.edu, tosun@fiu.edu

ABSTRACT
The results of a continuation of the existing novel prototype for robotic eye examination is presented. This work is the next step from the Teleoperated Ophthalmic Examination Robot in implementing a full remote ophthalmic diagnostic and treatment device.

Keywords
Slit lamp, robotic surgery, remote ophthalmology, telemedicine.

1. INTRODUCTION

The Ophthalmic Robot is a motorized slit lamp that allows for remote operation from a computer interface. The project was initiated by ophthalmologist Dr. Austin Bach and the initial prototype was developed by Melissa Morris. This project is a continuation and improvement of Melissa Morris' preliminary work [1]. Figure 1 shows the prototype from the previous work.

Figure 1 – Previous Robotic Slit Lamp Prototype [1]

A slit lamp microscope consists of two components: an illumination system that shines a bright focal light through a slit of variable width or height, and a magnification system that is usually binocular. Slit lamps allow for close surface examination of the front of the eye and inspection of the interior of the eye with the use of auxiliary lenses [2]. All major instrument manufacturers produce a range of slit lamps, though the basic principles remain the same for whichever model is selected [3]. Slit lamps can have the illumination system either above the magnification system or below. The slit in the illumination system can be adjusted on most slit lamp models. A practitioner should be able to adjust slit width and height while also being able to orient the slit horizontally and vertically. For easy movement of the slit lamp, most have a joystick installed and a locking device to hold it in position [3].

Modern slit lamps allow for photography of the eye, which allows for an accurate and consistent means for eye exam record keeping. Photographic capabilities can also allow for remote examinations where the practitioner does not need to be present with the patient. Traditionally, the most frequently used option for image capture of the anterior segment involves the use of a photographic slit lamp with a beam splitter attached to a 35mm camera back. Conventional 35mm photography requires adjustments to achieve the correct exposure. Recent advances in video cameras, image-capture boards, digital still cameras, and color printers has resulted in a more affordable and easier to use digital imaging where the major advantage of such systems is the ability to generate instantaneous images on a computer monitor [3].

2. MOTIVATION

Many people around the world are affected by some degree of visual impairment and seek corrective ophthalmic assistance [1]. Because ophthalmic operations are complex and risky, robotic technology can greatly assist with such procedures. When operating manual devices, physician fatigue becomes a factor as such work produces mental and physical wear. An ophthalmic robot can be controlled and monitored remotely by an ophthalmologist from almost any location with a potentially higher degree of precision. Though the overall cost savings may be questionable, there are some aspects of robotic technology that can provide economic benefits. It could be more cost efficient to develop a robotic slit lamp out of an existing slit lamp rather than designing a robot slit lamp from scratch because many older models are in use throughout the world. By using an established mounted motor retrofit system, an ophthalmologist could select which ever

slit lamp that suits his/her preferences. While the Ophthalmic Robot can be moved, traveling with the robot could potentially be costly [1].

3. EVALUATION OF FIRST PROTOTYPE

The previous robot was outfitted with four motor systems to control slit height and width, lens rotation, and slit lamp rotation. The robot was mounted onto a motorized platform allowing for planar movement of the entire structure. The motorized systems are mounted onto an existing slit lamp to allow for a major cost cut and to reduce FDA testing time. Figure 2 displays the four slit lamp adjustment systems and the motorized movement platform.

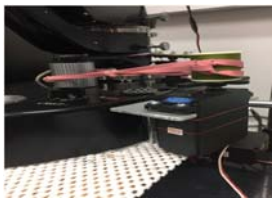

Slight Height Adjustment

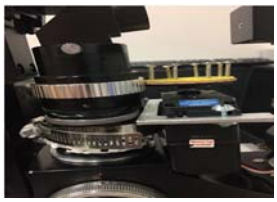

Slit Width Adjustment

Lamp Rotation

Lens Rotation

Omni-wheel Platform

Figure 2 – Previous Prototype Motor Systems

For improvement of the existing prototype, the existing motor systems were evaluated and revamped. There are five main constituents that made up the entire prototype. Firstly, there is a base comprised of four Omni-wheels and two motors that the slit lamp rested on, allowing it to move in the X and Y directions. The other four constituents were small systems composed of a motor and either a friction disk or band, allowing for the alteration of settings of the slit lamp, by rotation of an adjustment knob. The settings that these systems controlled were the slit height, lens rotation, lamp rotation, and slit width.

With all five of these components, there were a few imperfections and deficiencies. Regarding the Omni-wheel base, the system was too convulsive. This was due to a combination of the contour of the wheels, the rotation motors for the wheels, and the existing slit lamp track structure being warped from age and wear. As this instrument is used for eye examinations, smoothness is required.

The system that controlled the slit height was composed of a motor that is affixed to the slit lamp via metal brackets which rotates a spool. Linked rubber bands wrapped around the lamp's adjustment knob and the driver spool acted as a belt, thus rotating the knob. It was determined that system was in working order and the slit height knob worked as intended.

The system that controls the slit width was composed of a friction disk that is in tension with the slit width knob. Similar to the knob that adjusts the slit lamp's height, the light beam width was controlled by a completely circular dial. There was a motor mounted close to the lamp, and as a result a disc, rather than a belt, was intended to rotate the dial by friction. However, a sufficient amount of kinetic friction was not always created in order to adjust the knob consistently and inconsistencies in the knob actuation made the problem more prominent.

The two rotation systems that rotated the micrsocope and the lamp featured two motors bracketed to the back of the slit lamp. Each used disks to drive rotation of one of the arms. Both disk drives facilitated rotation, however the disks' friction surfaces degraded rather quickly, creating slippage. The contour at the back of the slit lamp is straight for the micrscope rotation system, but the contour slopes for the lamp rotation area. This results in a small amount of contact with the slit lamp, a crucial element in friction drives.

4. REVAMPED PROTOTYPE

The previous prototype was redesigned where a new movement platform was implemented and all four of the systems that control the position and settings of the slit lamp were replaced. Although the existing prototype provides a solid working foundation, there was room for improvement. The new designs give the existing prototype a cleaner look and improved performance.

4.1 PROPOSED DESIGNS

Starting with the movement platform, a motorized screw stepper motor stage was developed. The XY stage works by running the stepper motors mounted onto a rail system. The motors used are Haydon 28000 Series 11 Stepper Motor Linear Actuators, shown in Figure 3.

Figure 3 – Stepper Motor Linear Actuator

The slit lamp rested on top of a moving platform and the platform rests on top of eight 0.5in ball bearings. The ball bearings rolled as the motor applies a force on the motor and the adjacent motor slides along the rail. The key focal points of this design were that the weight of the slit lamp rests on the bottom platform, the screw stepper motors allow for a smooth and controlled movement, and the railing system keeps the moving platform in place and moving only in the X and Y directions. Figure 4 shows the SolidWorks model of the XY stage design.

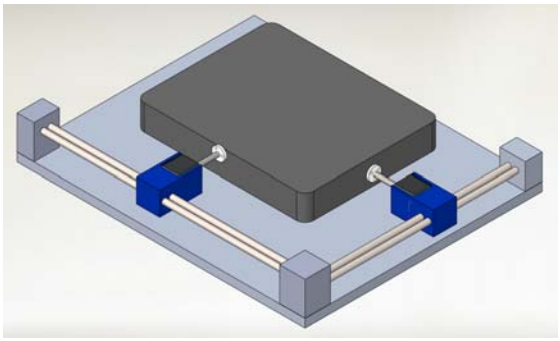

Figure 4 – Proposed XY Stage Design (SolidWorks)

For the four mounted motor systems, the previous motors used on the first prototype was replaced with identical Turnigy Servo motors, shown in Figure 5. The Turnigy servo motors provide ample torque and allow for a variety of mounting options.

Figure 5 – Turnigy Servo Motor

For the two rear-mounted arm rotation systems, gear drives were used to rotate the microscope and illumination system. Gear drives were selected because they do not require a pre-load that a friction drive requires. This results in easier mounting and a higher degree of precision. Circular gear racks were attached to the slit lamp itself and pinions will be attached to the motors. The pinions were the driving forces behind the rotational motion. Figure 6 displays the designs, modeled in SolidWorks, for the illumination system rotation and the lens rotation.

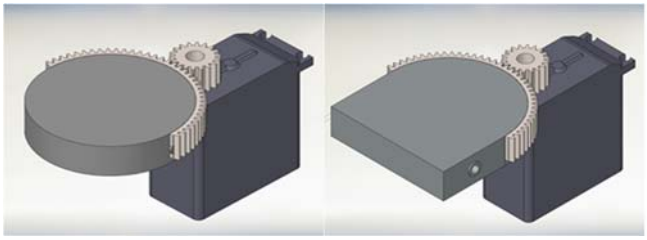

Figure 6 – Lamp Rotation (Right) and Lens Rotation (Left)

For the slit height adjustment, it was decided to keep the belt concept, but improve the belt system. The existing prototype's rubber band setup performed at a satisfactory level, therefore no major change was needed. In the new design, a different belt was used and a pulley was 3D printed for this system. For the slit width adjustment, it was decided to replace the existing friction drive with a belt drive. Similar to the slit height adjustment, a pulley was manufactured for the system. A gear drive was the ideal option, but difficulty in mounting the gear onto the knob was the main deterant. Figure 7 shows the SolidWorks models of both systems.

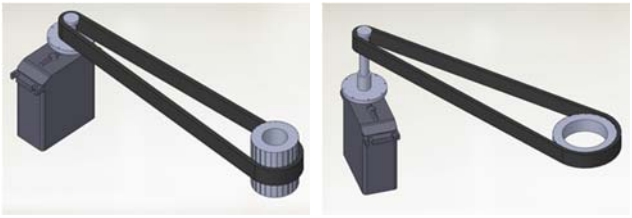

Figure 7 – Slit Height (Left) and Slit Width (Right) Designs

4.2 ENGINEERING DESIGN

Stress tests and several structural analyses of the XY stage were conducted to ensure that the stage is capable of safely holding the weight of the slit lamp, withstanding the reaction force of the motors, and that movement occurs. For the gear drives used for the rotation systems, calculations were performed to determine if the selected gears experience any interference.

4.2.1 Slit Lamp XY Stage Static Friction

The maximum thrust force that the stepper motors can produce onto the slit lamp platform is 25lbs. The static friction force of the slit lamp and platform must be less than 25lbs for the system to move from rest. The force needed to keep the system in motion is less than the static friction force.

$$F_{motor} > \mu_{static} W_{system}$$

The maximum weight of the slit lamp and its components is 30lbs and the maximum possible weight of the slit lamp platform and ball bearings is 10lbs. The friction coefficient noted is between the stainless-steel ball bearings and the surface of the bottom platform. For a maximum possible system weight of 40lbs and a worst-case scenario friction coefficient of 0.6, the motor needs to provide a force of at least 24lbs to get the system to move. Steps can be taken to reduce the friction coefficient such as using a lower coefficient of friction material combination and by using lubricant. Table 1 displays friction coefficients for possible base material combinations for dry and clean environments.

Table 1. Friction Coefficients for Material Combinations

Material Combination		Static Coefficient of Friction
Stainless Steel	Aluminum	0.45
Stainless Steel	Wood	0.2 – 0.6
Stainless Steel	Plastic	0.25 – 0.4

4.2.2 Motor Reaction Force and Rod Design

While the maximum force that the motor can exert onto the slit lamp platform is 25lbs, the rods supporting the motor and mount had to withstand the reaction force that the motor applies on the platform. If the rods could not hold the reaction force, the platform would not move. A stress analysis was conducted by taking a distributed 25lb load on the middle on the longer rod where 14in of the 15in rod is exposed. The distributed load was 1.375in located at

the middle of the rod, as a worst-case scenario as shown in Figure 8.

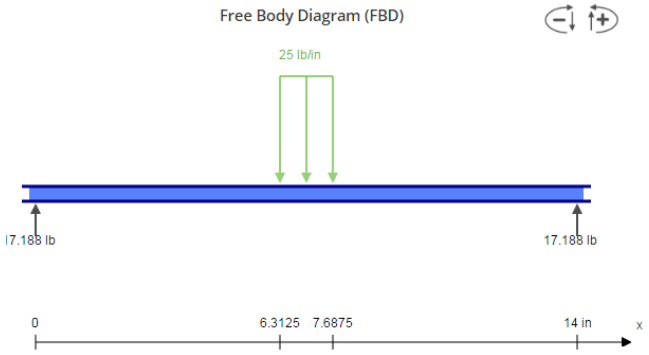

Figure 8 – Free Body Diagram of Reaction Force on Rod

Shear force and bending moment diagrams were created to perform a Von Misses failure analysis. The minimum diameter required to hold the motor reaction force was calculated for stainless-steel, steel, and aluminum with an arbitrary factor of safety of 1.25. Once a rod diameter of 5/16in was decided, the factor of safety and maximum rod deflection were calculated. Table 3 displays the results of these calculations.

Table 2. Rod Design Analysis Results

Material	Yield Strength	Minimum Diameter	Factor of Safety
Aluminum	13.8 kpsi	0.482 in	0.361
Stainless Steel	72.8 kpsi	0.271 in	1.91
Steel	50.0 kpsi	0.308 in	1.31

Though the 25lb motor reaction force was a worst-case situation, it is important to use rods that withstand this scenario. Aluminum does not perform well under the 25lb reaction load as it fails and undergoes a large deflection of 0.420in, therefore it should not receive consideration for the rod material. Stainless steel and regular steel work fine, but still undergo deflection. Though both stainless and regular steel both work as the rod material, stainless steel was the recommended material.

4.2.3 Gear System Interference

The smallest number of teeth were calculated for both the driver pinion and the circular gear rack. If the selected gears have a tooth count smaller than the smallest allowable amount, interference occurs. Interference occurs when the contact of portions of tooth profiles are not conjugate [4]. A spur gear set of 24 diametral pitch and 20° pressure angle was selected. The circular gear rack had a pitch diameter of 3in with 72 teeth and the pinion had a pitch diameter of 1.25in with 30 teeth. The following equations were used to calculate smallest allowable tooth sizes where *m* is the tooth ratio of the gear and pinion. Both the selected pinion and gear satisfy this interference criteria.

$$N_P = \frac{2k}{(1+2m)sin^2\phi}\left(m + \sqrt{m^2 + (1+2m)sin^2\phi}\right) = 7.5T$$

$$N_G = \frac{N_P^2 sin^2\phi - 4k^2}{4k - 2N_P sin^2\phi} = 33.5T$$

4.2.4 Stress on Platform and Rod Towers

The slit lamp platform for the XY stage of the Ophthalmic Robot wias used to transport the slit lamp in both the X and Y directions. It was powered by the stepper motors referenced earlier in the report. This 10in by 8in platform was supported by eight steel balls 0.5in in diameter. SolidWorks Simulation determined that the platform was able to sufficiently support the weight of the slit lamp without the platform buckling. To take into account cost efficiency and weight of the base, different alternatives for which to build the base were examined. These alternatives included ABS plastic, aluminum, and oak wood. For the simulation, a 25lb distributed load in the shape of the slit lamp's bottom platform acted on top of the platform. The platform rests on the eight stainless steel ball bearings noted above. It was intended, that as the slit lamp is resting on the platform or while in use, that weight is evenly distributed across that designated area. The maximum stress acting on the platform during the simulation was noted as approximately 13.4psi. This with a very low amount of stress produced high factors of safety. The weight of the slit lamp produced a compression force on the platform, which resulted in a low possibility of failure. It was determined that the platform could be made out of all three considered materials. Figure 9 displays the stress distribution acting on the platform. The stainless-steel ball bearings support the load.

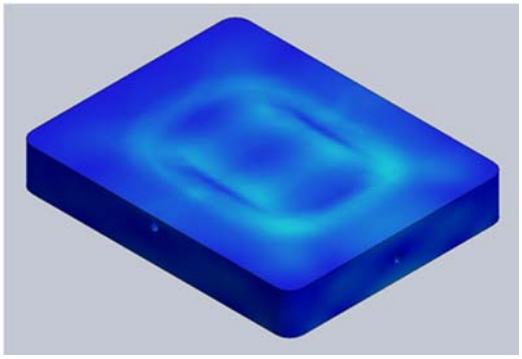

Figure 9 – Slit Lamp Platform Stress Distribution

A static study was conducted in SolidWorks Simulation to test the structural integrity of the brackets that supported the rods above the table. The bottom of the brackets were fixed to emulate it being attached to the bottom platform. The reaction forces from the free body diagram at the end of each support was used in the bracket static study. The result of the simulation indicated that the maximum stress was 296.7psi. The maximum stresses occured inside the holes where the rods act on it and at the bottom corner of the bracket. Figure 10 displays the stress distribution on each rod bracket tower. This result indicates that the brackets can be made out of most materials with the primary options being aluminum, ABS plastic, and wood.

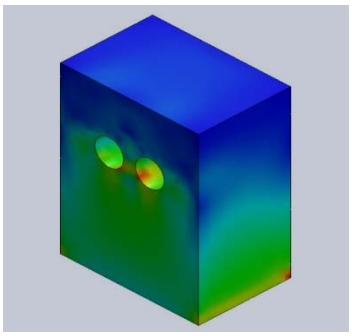

Figure 10 – Stress Distribution on the Rod Brackets

4.3 PROTOTYPE CONSTRUCTION

For the XY stage, the slit lamp sat atop a moving wooden platform that rolled on eight stainless steel ball bearings. As the platform was pushed by the linear stepper motors, the ball bearings rolled, allowing for ease of movement. The platform was capable of moving in both lateral directions. The linear stepper motor lead screw nuts were glued to the outside of the drilled holes in the sides of the moving platform. The stepper motors rested inside of 3D printed mounts that slid along steel rods. The rods were supported by wooden rod bracket towers at the ends of the bottom platform where everything rested. Each motor mount was meant to slide as the other motor was in motion. Figure 11 shows the constructed XY stage.

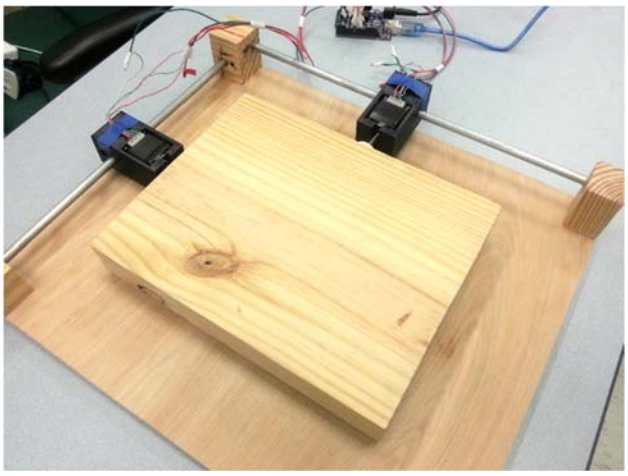

Figure 11 – XY Stage Assembly

Once the design phase was completed, the prototyping process was carried out. Due to cost constraints, a decision was made to make the XY stage out of wood. Wood is a cheap alternative to machined aluminum and can withstand many possible structural stresses that may act on it. Many other components of the Ophthalmic Robot were 3D printed with PLA thermoplastic. The other components that could not be 3D printed were bought. Such components include the motor mount rods, stainless steel ball bearings, the drive belts, and all motors used.

Construction of the slit lamp motor systems became an assembly operation once the pulleys, gears, and mounts were 3D printed. For the slit height and slit width motor systems, the servo motors were attached to the sides of the slit lamp using a combination of metal brackets and hose clamps. The pulleys were attached to the servo motors and the belts were cut to size out of the friction tape. The friction tape was then tensioned and connected together to create the belt drives. Figure 12 shows the revamped slit height motor system and Figure 13 shows the revamped slit width motor system.

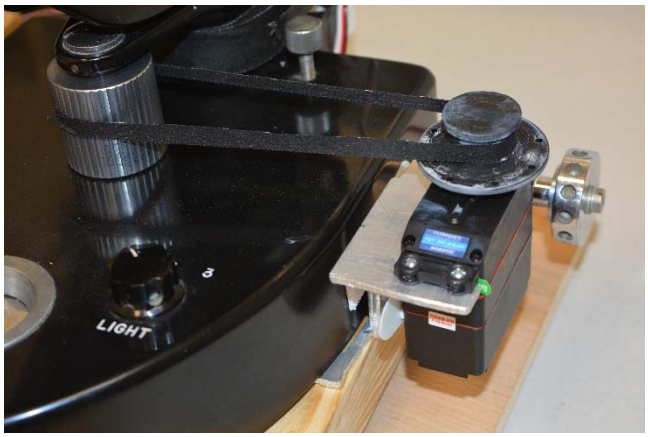

Figure 12 – Revamped Slit Height Motor System

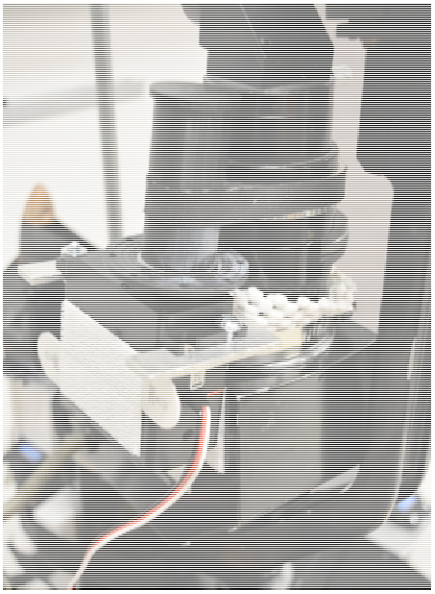

Figure 13 – Revamped Slit Width Motor System

For the microscope and lamp rotation motors, a lower motor mount was first attached to the back bottom of the slit lamp. The magnification system rotation motor was attached to the mount with 3mm double-sided tape. The circular gear racks were glued to the slit lamp and the pinion gears were attached to the servo motor output shafts. Care was taken to ensure that the gear meshed with the circular gear rack. For the illumination system rotation motor, two 3D printed brackets were used to connect it to the magnification system rotation motor underneath it. The upper motor was inverted and the gear was meshed with the circular gear

rack. Figure 14 shows the revamped lens rotation system and lamp rotation system.

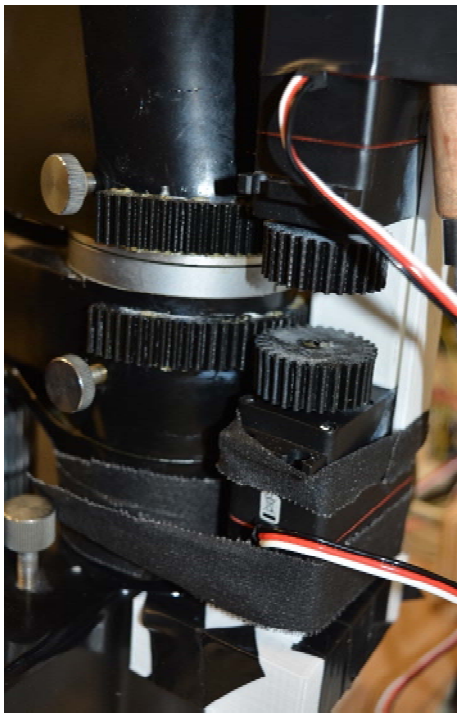

Figure 14 – Revamped Lens Rotation and Lamp Rotation

The servo motors were all connected to an Adafruit servo shield that had an external source powering the motors. The stepper motors were connected to stepper drivers on a breadboard with an external 12V power source powering the motors. The servo shield and the stepper motors were connected to a BeagleBone Black that was used as the primary controller. The same software used for the first prototype was used in the controller with updates made to accommodate the stepper motor and XY stage. Figure 15 shows the completed setup of the Ophthalmic Robot and the computer interface.

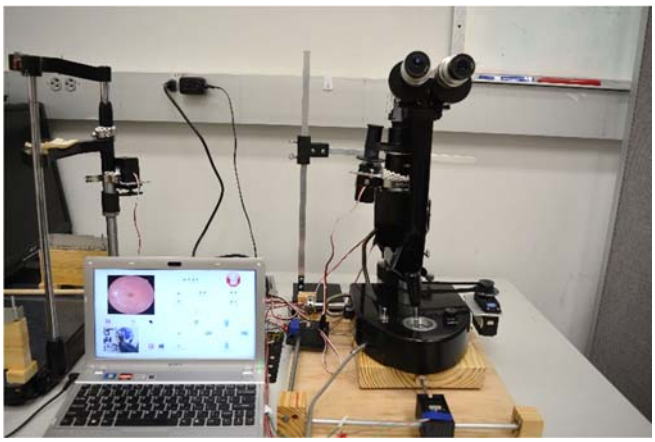

Figure 15 – Ophthalmic Robot and Computer Interface

5. RESULTS

After assembling the XY stage and mounting the servo motors, the design was tested by running the motors and seeing if the platform moves as intended. After checking the movement of the motor mounts of the XY stage, it was necessary to remove a rod from each railing to give the mounts free movement. The holes of the rod towers did not line up perfectly due to manufacturing constraints, so having two parallel rods for each direction was not feasible. Once the motor mounts could move freely, the motors were run to test the movement of the platform. The platform was able to move in the two directions, both horizontally and vertically. When given the required 12V power source, the motors were able to provide movement to the platform with the slit lamp on top of it at a slow pace of approximately 1mm/s. Despite this slow pace, there are a few advantages. The slit lamp is a delicate instrument that would require a slow acceleration and slow deceleration to be able to move without tipping over. The slow pace also allows the doctor controlling it to accurately position the slit lamp without having to worry about overshooting the intended position.

The slit lamp adjustment systems were each tested to see if they rotated their assigned knob or position. For the slit height and slit width adjustment systems, the friction belts in each system rotate the knobs as intended. They both work at varying motor rotation speeds and in small increments. For the lens rotation system and illumination rotation system, both motors were tested to see if both entities rotate as designed. Both systems rotate smoothly due to the gear pinions and circular gear racks being in mesh and having good contact to provide smooth rotation. Some work can be done in the future to improve the rear servo mounting brackets, however, as they have a tendency to move away from the slit lamp in some instances. Friction tape would ideally also be replaced by custom-sized rubber or silicone belts as the tape must be adjusted and replaced frequently.

Due to the nature of this project, the testing done was more on a trial and error basis. This is because the motors can be controlled to go at any speed within their capabilities. The performance of the motor systems heavily relies on the programming. The main testing that was done was checking if the motor systems run properly through the computer interface and contact between the motor systems and the slit lamp was adequate.

6. ACKNOWLEDGMENTS

David Larsson, Daniel Irving, Shehryar Effendi, and Joshua Dubin would like to thank Ph.D. candidate Melissa Morris and Dr. Sabri Tosunoglu for providing support and guidance throughout the duration of this project. They would also like to thank Lars-Erik Larsson for his much appreciated assistance in the construction of the XY stage movement platform. Finally, the authors extend their thanks to Dr. Austin Bach of TYB, Inc. for providing financial support for the first iteration of this project.

7. REFERENCES

[1] Melissa Morris, Sabri Tosunoglu, “Teleoperated Ophthalmic Examination Robot,” Florida International University, Miami, FL, May 2016.

[2] College of Optometrists Associates, “Slit Lamps,” College of Optometrists [Online], United Kingdom, 2016. Available: http://www.collegeoptometrists.org/en/college/museyeum/online_exhibitions/optical_instruments/slit_lamps.cfm

[3] Jane Veys, John Meyler, Ian Davies, “Slit-lamp Examination,” Johnson and Johnson Vision Care Institute [Online], 2016. Available: https://www.jnjvisioncare.co.uk/sites/default/files/public/uk/tvci/eclp_chapter_2.pdf

[4] Richard G. Budynas, J. Keith Nisbett, “Shigley’s Mechanical Engineering Design Tenth Edition,” McGraw-Hill Education, New York, NY, 2015.